Improved visible-light activities of nanocrystalline CdS by coupling ultrafine NbN with lattice matching for hydrogen evolution

Yang Qu[a], Ning Sun[a], Muhammad Humayun[a], Amir Zada[a], Ying Xie[a], Junwang Tang[b], Liqiang Jing[a]* and Honggang Fu[a]*

Metallic ultrafine NbN with lattice matching to nanocrystalline CdS could replace the expensive platinum for efficiently trapping photogenerated electrons, enhancing charge separation and then catalyzing the preferentially absorbed H_2O to produce H_2, mainly confirmed by Kelvin probe, Mott-Schottky plot, produced •OH amount, electrochemical experiments and density-functional-theory theoretical calculations.

Semiconductor-based photocatalytic hydrogen production by solar energy has been considered to be one of the most significant approaches to solve the worldwide energy crisis.[1-3] It is widely accepted that semiconductor materials play a vital role in photocatalysis. An ideal semiconductor photocatalyst has to possess broad-spectrum light harvesting, effective charge separation and efficient surface catalytic/active capacity. Over the past few decades, great attentions have been focused toward the synthesis of efficient photocatalysts and the study of photocatalytic mechanism.[4-6] However, the efficiencies of photocatalytic hydrogen production for state-of-the-art works is still unsatisfactory for industry due to several shortcomings of the semiconductor photocatalysts, especially the sluggish charge separation and poor surface activation.[7-10]

CdS with suitable electronic bandgap (Eg=2.4 eV, with conduction band at -0.52 eV vs NHE) is ideal semiconductor for photocatalytic H_2 evolution.[11] However, the shortcomings of the sluggish charge separation and poor surface activation of H_2O result the poor photocatalytic activity for H_2 production. [12] It is therefore much meaningful to synchronously enhance the charge separation and improve the surface activation of H_2O so as to promote the photocatalytic activity of CdS. Usually, platinum (Pt) is widely used as a co-catalyst to enhance the charge separation through the formed Schottky barrier and promote the surface catalytic capacity *via* its natural catalytic ability. [4,13,14] However, the expensive price and resource shortage limit the practical applications of Pt. Therefore, new substituents are eagerly needed. Although some metallic transition metal sulfides and carbides, such as WS_2, MoS_2, MoB_2 and WC, are tried, the H_2 production activities are still unsatisfied owing to the poor charge transferring across the mismatched lattices interface and weak absorption of H_2O on their surfaces.[15-18] As a consequence, new materials having matched lattices with CdS are still required. Emphatically, the lattice matching of two different components in heterojunctions is much important for charge separation.[19,20]

Niobium nitride (NbN) is metallic as well-known superconductor and has been considered to be one of the promising cryoelectronic materials.[21] Significantly, it has similar crystal lattices as that of CdS, along with the perfect matched lattices. As shown in Figure S1, density functional theory (DFT) reveals that the (002) lattice plane of NbN and CdS is only 0.03% mismatched, which is more advance than (002) Pt/CdS (1.5% mismatched). Moreover, NbN is reported to be metallic with low work function, suggesting it be the rational candidate to improve the photocatalytic activity of CdS for H_2 production.[22] To date, there is seldom works focusing on the NbN/CdS nanocomposites for photocatalysis.

Hence, we report an interesting NbN/CdS nanocomposites for photocatalytic hydrogen production under visible light irradiation. Nanocrystalline NbN was synthesized by ammonolysis method. CdS nanocrystallite was grown in the presence of NbN *via* chemical bath deposition method to prepare NbN/CdS nanocomposites (see Electronic Supplementary Information). XRD in Figure S2 shows the five Bragg diffraction peaks of bulk NbN which are in good agreement with the standard card (JCPDS No.89-6042, a=b=4.107027Å).[23] Raman spectra (Figure S3), also confirm the preparation of pure-phase NbN.[24] The diffraction peaks of the bare nanocrystalline CdS are well matched with the standard card (JCPDS No.41-1049, a=b=4.10829Å). XRD and Raman spectra demonstrate the successful preparation of NbN/CdS nanocomposites.

SEM image (Figure S4) and TEM image inset Figure 1 A demonstrate that the average diameter of as-prepared ultrafine NbN nanocrystallite is approximately 30 nm. HRTEM image (Figure 1A) reveals that the lattice fringes with d-spacing (d=0.22 nm) correspond to the (002) crystallographic planes of ultrafine NbN.

a. *Key Laboratory of Functional Inorganic Materials Chemistry (Heilongjiang University), Ministry of Education, School of Chemistry and Materials Science, International Joint Research Center for Catalytic Technology, Harbin 150080, P. R. China. E-mail: jinglq@hlju.edu.cn; fuhg@hlju.edu.cn*
b. *Department of Chemical Engineering, University College London, Torrington Place, London WC1E 7JE, UK. E-mail: Junwang.tang@ucl.ac.uk*
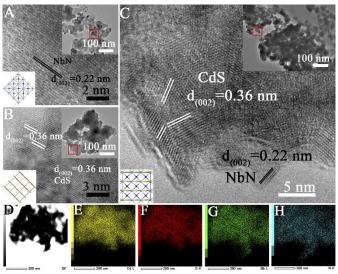
Figure 1 TEM and HRTEM of bare NbN (A), bare CdS (B) NC-1 (C) and TEM mapping of NC-1 (D) (four element Cd (E), S (F), Nb (G),N (H) can be observed). The insets of A, B and C show the low resolution TEM images of the corresponding samples.

The average diameter of bulk nanocrystalline CdS is 5-10 nm as shown in Figure 1B with serious aggregation (inset Figure 1B). TEM image of NbN/CdS nanocomposites (NC-1) inset Figure 1C reveals that the dispersion of CdS nanocrystallites is improved after coupling ultrafine NbN. The lattice fringe at (002) plane with d-spacing 0.22 nm in HRTEM image (Figure 1 C) corresponds to NbN while the latter at (002) plane with d-spacing 0.36 nm is attributed to CdS. TEM mapping of NC-1 (Figure 1D), reveals that the nanocomposite is made up of contributions from each element i.e. Cd (Figure 1E), S (Figure 1F), Nb (Figure 1G) and N (Figure 1H), exhibiting a high dispersion of ultrafine NbN and well contact of NbN and CdS in the nanocomposites. XPS in Figure S5A further demonstrates the chemical composition of CdS and NbN. The high resolution XPS (Figure S 5B and 5C) shows that the peak position of S in nanocomposite slightly shifts toward higher binding energy compared to the bare CdS while that of Nb shifts toward lower binding energy revealing that the heterojunction between NbN/CdS nanocomposite has been formed. The well lattices matched (002) NbN and (002) CdS is favorable to the charge separation, leading to promoted photocatalytic activity.

Figure 2A shows the photocatalytic H_2 evolution activities of various samples. The photocatalytic activity of mechanically mixed sample MNC-1 further reveals that coupling of NbN is feasible. One can see that the photocatalytic activity of nanocrystalline CdS is obviously promoted after coupling small amount of NbN. NC-1 exhibits the optimal photocatalytic activity under visible light irradiation for 1h, which is up to 126 μmol over 0.1g catalyst. If the amount of NbN is increased continuously, its black color affects the light absorption of CdS (Figure S6), which results in a lower activity. The time course H_2 evolution activities (Figure S7) show that the samples are good and continuous. Importantly, the photocatalytic activity of NC-1 is obviously 1.4-time higher than that of 1wt% Pt -CdS (90 μmol over 0.1g catalyst). Moreover, the apparent quantum efficiency (QE) of NC-1 (2.2%) is higher than 1wt% Pt/CdS (1.5%) at 420 nm. Compared to Pt/CdS, NC-1 also exhibits long

time stability for six successive photocatalytic recycles in 24 h, suggesting that the NbN/CdS nanocomposites of NC-1 are highly stable (Figure 2B). The stability is further confirmed from measuring the concentration of Cd^{2+} in the solution after 12 h irradiation by atomic absorption spectrometry, as shown in Table S1. From N_2 adsorption-desorption isotherms (Figure S8), it is clear that the surface area is hardly attributed to the promoted photocatalytic activity. The promoted photocatalytic activity of NC-1 could be attributed to the well matched lattices to enhance charge separation. Comparison of the photocatalytic activities in Figure S9 clearly demonstrate that the lattice matching positively affects the photocatalytic activities.
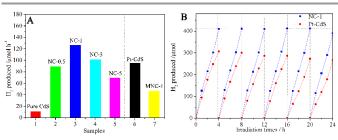

Figure 2 Photocatalytic H_2 production activities of different samples (A) and stability of NC-1 and 1 wt% Pt/CdS in 24h continuous photocatalytic recycles for H_2 production (B).

Besides, there are other reasons for the enhanced charge separation in NbN/CdS nanocomposites. DFT theoretical calculations of the partial density of states for NbN show all the electron orbits across the Fermi level plane (Figure S10), suggesting that NbN is metallic as it was reported.[25] Additionally, the work functions of the Pt, NbN, CdS, and NC-1 are about 5.25, 5.18, 4.6 and 5.06 eV, respectively as measured from Kelvin probe (Figure 3A). The metallic NbN possesses lower Fermi level than that of CdS, suggesting it be an electron collector in the NbN/CdS heterojunctional nanocomposite. Remarkably, the contact potential difference (CPD) of NbN/CdS is 70 mV smaller than that of Pt/CdS, implying that the lower energy barrier between CdS and NbN is much small for charge transferring.[26] To further confirm the charge separation, the coumarin fluorescent method was used to detect the amount of produced hydroxyl radicals (·OH), in which the coumarin could easily react with the formed ·OH and produce luminescent 7-hydroxy-coumarin. As demonstrated earlier, the ·OH amount could effectively reveal the separation of photogenerated charges in the photocatalysis.[27] As expected, it is confirmed according to Figure 3B that the ·OH amounts produced by NC-1 are much obvious as compared to those by the bare CdS and NbN. Hence, it is deduced that the increase in the amount of coupled NbN is directly related with the enhanced the charge separation.

Carrier density (N_d) of semiconductors is a significant parameter to measure the charge separation in heterojunctions.[28] The N_d can be calculated from the slope of the Mott-Schottky plot using the following equation:[29]

$$N_d = (2/e_0 \varepsilon \varepsilon_0)[d(1/C^2)/dV]^{-1}$$

Where e_0 is the electron charge, ε is the dielectric constant, $ε_0$ is the permittivity of vacuum, N_d is the carrier density and V is the applied bias at the electrode. It is thus the slope of the Mott-Schottky plot that reveals the carrier density, with inversely proportional relationship. From Figure 3C, the NC-1 shows smaller slope of the Mott-Schottky plot compared to the CdS nanoparticles, suggesting a high carrier density at the contacted interface. While the smaller arc belongs to NC-1 in middle frequency of electrochemical impedance spectroscopy (EIS) in Figure 3D demonstrates that the interfacial resistance becomes much lower after coupling NbN with CdS, favoring charge transfer and separation. Mott-Schottky plot and EIS confirm that the interface of NbN and CdS favors charge transfer and separation. This can be further supported by photoluminescence spectra in Figure S11.
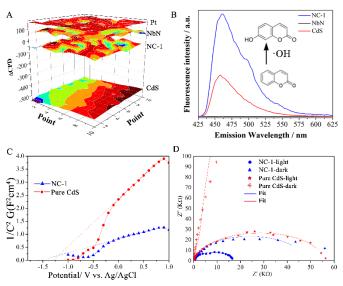
Figure 3 Scheme of Kelvin probe of Pt, CdS, NbN and NC-1 (A) and fluorescence spectra related to the produced •OH amount by coumarin trapping method of CdS, NbN and NC-1(B), Mott-Schottky plots of CdS and NC-1 (C) and EIS of CdS and NC-1 in dark and under visible light irradiation (λ>420 nm) (D) .

As the consequent step of charge separation, the adsorption and activation of H_2O on the surface of photocatalyst is much crucial for the photocatalytic activity of H_2 reduction.[30,31] However, the surface photochemical mechanism of NbN is so far unclear and seldom concerned previously. As for this, the adsorption and activation of H_2O on the surface of the optimal NbN/CdS nanocomposite was studied. Theoretical calculations *via* DFT inset Figure 4 show that the adsorption energy of water molecule on (002) NbN is -1.8 eV, while it is -0.5 eV for (002) Pt, demonstrating that NbN possesses strong adsorption for H_2O on its surface. Thus, H_2O is more favorable to be adsorbed on NbN revealing that NbN is appropriate for photocatalytic hydrogen production, in particular after coupling with lattice-matched CdS. Further, electrochemical water reduction was carried out as shown in Figure 4. The reductive current of NC-1 is -0.76 mA/cm² which is much closer to that of 1 *wt.*% Pt/CdS (-0.78 mA/cm²) at the potential of -1.2 V (Ag/AgCl). These electrochemical properties reveal that, NbN could act as a co-catalyst to effectively catalyze hydrogen production by the collected photogenerated electrons.
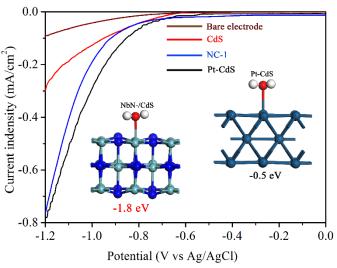
Figure 4 Electrochemical hydrogen reduction curves of bare electrode, CdS, NC-1 and Pt/CdS with inset showing the adsorption energies of H_2O on (002) NbN and (002) Pt.

In summary, NbN/CdS nanocomposites were prepared for high efficiency photocatalytic hydrogen production which was 10-time and 1.4-time higher than bulk CdS and Pt/CdS respectively, and displayed high stability even after six successive photocatalytic recycles. It was demonstrated that the promoted photocatalytic activity could be attributed to the matched lattices and formed heterojunctions between metallic NbN and CdS. Emphatically, in this work, NbN as a new type of co-catalyst favors to trap the photogenerated electrons from CdS to efficiently react with the preferentially absorbed water on NbN to effectively produce hydrogen gas.

References

1   S. J. A. Moniz, S. A. Shevlin, D. J. Martin, Z. X. Guo and J. Tang, *Energy Environ. Sci.*, 2015, **8**, 731

2   T. Hisatomi, J. Kubota and K. Domen, *Chem. Soc. Rev.*, 2014, **43**, 7520.

3   K. Maeda and K. Domen, *B. Chem. Soc. Jpn.*, 2016, **89**, 627.

4   J. Yang, D. Wang, H. Han and C. Li, *Acc. Chem. Res.*, 2013, **46**,1900.

5   X. Fan, X. Wang, W. Yuan and C. M. Li, *Sustainable Energy Fuels*, 2017, **1**, 2172-2180.

6   S. Xie, Q. Zhang, G. Liu and Y. Wang, *Chem. Commun.*, 2016, **52**, 35.

7   J. Liu, Y. Liu, N. Liu, Y. Han, X. Zhang, H. Huang, Y. Lifshitz, S. T. Lee, J. Zhong and Z. Kang, *Science*, 2015, **347**, 970.

8   R. Shi, Y. Cao, Y. Bao, Y. Zhao, G. I. N. Waterhouse, Z. Fang, L. Z. Wu, C. H. Tung, Y. Yin and T. Zhang, *Adv. Mater.*, 2017, **29**, 1700803

9   Y. Ma, X Wang, Y Jia, X. Chen, H. Han and C. Li, *Chem. Rev.*, 2014, **114**, 9987.

10 L. Liao, Q. Zhang, Z. Su, Z. Zhao, Y. Wang, Y. Li, X. Lu, D. Wei, G. Feng, Q. Yu, X. Cai, J. Zhao, Z. Ren, H. Fang, F. Robles-Hernandez, S. Baldelli and J. Bao, *Nat. Nanotechnol.*, 2014, **9**, 69.

11 X. Wang, L. Yin and G. Liu, *Chem. Commun.* 2014, **50**, 3460.

12 L. Jiang, L. Wang, G. Xu, L. Gu and Y. Yuan, *Sustainable Energy Fuels,* 2018, http://dx.doi.org/10.1039/C7SE00475C.

13 S. Bai, J. Jiang, Q. Zhang and Y. Xiong, *Chem. Soc. Rev.* 2015, **44**, 2893.

14 Y. Qu and X. Duan, *Chem. Soc. Rev.*, 2013, **42**, 2568.

15 J. Chen, X. J. Wu, L. Yin, B. Li, X. Hong, Z. Fan, B. Chen, C. Xue and H. Zhang, *Angew. Chem. Int. Ed.*, 2015, **54**, 1210.

16 P. R. Jothi, Y. Zhang, J. P. Scheifers, H. Park and B. P. T. Fokwa, *Sustainable Energy Fuels,* 2017, **1**, 1928-1934.

17 J. S. Jang, D. J. Ham, N. Lakshminarasimhan, W.Y. Choi and J. S. Lee, *Appl. Catal. A-Gen.*, 2008, **346**, 149.

18 X. Zou and Y. Zhang, *Chem. Soc. Rev.*, 2015, **44**, 5148.

19 R. Li, F. Zhang, D. Wang, J. Yang, M. Li, J. Zhu, X. Zhou, H. Han and C. Li. *Nat. Commun.*, 2013, **4**, 1432.

20 S. Chen, S. Shen, G. Liu, Y. Qi, F. Zhang and C. Li, *Angew. Chem. Int. Ed.*, 2015, **54**, 3047.

21 A. Korneev, P. Kouminov, V. Matvienko, G. Chulkova, K. Smirnov, B. Voronov and G. N. Gol'tsman, *Appl. Phys. Lett.*, 2004, **84**, 5338.

22 R. Fujii, Y. Gotoh, M.Y. Liao, H. Tsujia and J. Ishikawa, *Vacuum*, 2006, **80**, 832.

23 N. Cansever, M. Danişman and K. Kazmanli, *Surf. Coat. Tech.*, 2008, **202**, 5919.

24 R. Kaiser, W. Spengle, S. Scricktanz and C. Politis, *Phys. Stat. Sol. (b)*, 1978, **87**, 565.

25 X. Liu, G. Zhou, S. W. Or, S. Ran and Y. Sun, *Ceram. Int.*, 2015, **41**, 849.

26 X. Zhang, Y. Lin, D. He, J. Zhang, Z. Fan and T. Xie, *Chem. Phys. Lett.*, 2011, **504**, 71.

27 Z. Li, P. Luan, X. Zhang, Y. Qu, F. Raziq, J. Wang and L. Jing, *Nano Res.*, 2017, **10**, 2321.

28 J. Shan, F. Raziq, M. Humayun, W. Zhou, Y. Qu, G. Wang and Y. Li, *Appl. Catal. B: Environ.*, 2017, ***219***, 10.

29 Q. Xu, J. Yu, J. Zhang, J. Zhang and G. Liu, *Chem. Commun.*, 2015, **51**, 7950.

30 X. L. Wang, W. Liu, Y. Y. Yu, Y. Song, W. Q. Fang, D. Wei, X. Q. Gong, Y. F. Yao and H. G. Yang, *Nat. Commun.*, 2016, **7**, 11918.

31 F. Zhang, A. Yamakata, K. Maeda, Y. Moriya, T. Takata, J. Kubota, K. Teshima, S. Oishi and K. Domen, *J. Am. Chem. Soc.*, 2012, **134**, 8348.